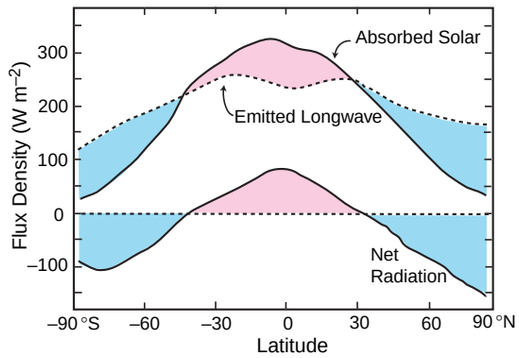

Fig. 10.2 Annual average flux density of absorbed solar radiation, outgoing terrestrial radiation, and net (absorbed solar minus outgoing) radiation as a function of latitude in units of W m^{-2}. Pink (blue) shading indicates a surplus (deficit) of incoming radiation over outgoing radiation. [Adapted from Dennis L. Hartmann, *Global Physical Climatology*, p. 31 (Copyright 1994), with permission from Elsevier.]

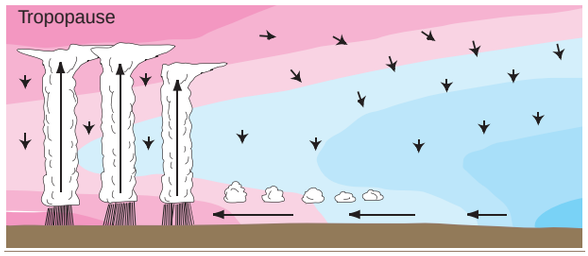

Fig. 10.3 Schematic of air parcels circulating in the atmosphere. The Colored shading represents potential temperature or moist static energy, with pink indicating higher values and blue lower values. Air parcels acquire latent and sensible heat during the time that they reside within the boundary layer, raising their moist static energy. They conserve moist static energy as they ascend rapidly in updrafts in clouds, and they cool by radiative transfer as they descend much more slowly in clear air.

The vertical distribution of temperature within the troposphere is determined by the interplay among radiative transfer, convection and large-scale motions. The radiative equilibrium temperature profile is unstable with respect to the dry adiabatic lapse rate. The pronounced temperature minimum near the 10-km level that defines the tropopause (Fig. 1.9) corresponds roughly to the level of unit optical depth for outgoing longwave radiation. Below this level, the repeated absorption and reemission of outgoing longwave radiation render radiative transfer a relatively inefficient mechanism for disposing of the energy absorbed at the Earth's surface. Convection and large-scale motions conspire to maintain the observed lapse rate near a value of 6.5 K km^{-1}.

The observed lapse rate is stable, even with respect to the saturated adiabatic lapse rate, because most of the volume of the troposphere is filled with slowly subsiding air, which loses energy by emitting longwave radiation as it sinks, as documented in Fig. 4.29. As the air loses energy during its descent, its equivalent potential temperature and moist static energy decrease, creating a stable lapse rate, as shown schematically in Fig. 10.3. It is only air parcels that have resided for some time within the boundary layer, absorbing sensible and latent heat from the underlying surface, that are potentially capable of rising through this stably stratified layer. Thermally direct large-scale motions, which are characterized by the rising of warm air and the sinking of cold air, also contribute to the stable stratification. It is possible to mimic these effects in simple *radiative-convective equilibrium* models by artificially limiting the lapse rate, as shown in Fig. 10.4. The tropospheres of Mars and Venus and the photosphere of the sun[2] can be modeled in a similar manner.

The concept of radiative-convective equilibrium is helpful in resolving the apparent paradox that greenhouse gases produce radiative cooling of the atmosphere (Fig. 4.29), yet their presence in the atmosphere renders the Earth's surface warmer than it would be in their absence. An atmosphere entirely transparent to solar radiation and in pure radiative equilibrium would neither gain nor lose energy by radiative transfer in the longwave part of the spectrum. However, it is apparent from Fig. 10.4 that under conditions of radiative-convective equilibrium, temperatures throughout most of the depth of the troposphere are above radiative equilibrium. It is because of their relative warmth (maintained mainly by latent heat release and, to a lesser extent, by the absorption of solar radiation and the upward transport of sensible heat by atmospheric motions) that greenhouse gases in the troposphere emit more longwave radiation than they absorb. Because the tropospheric lapse rate is determined not

[2] The sun's *photosphere* is defined as the layer from which sunlight appears to be emitted; i.e., the level of unit optical depth for visible radiation. The photosphere marks the transition from a lower, optically dense layer in which convection is the dominant mechanism for transferring heat outward from the nuclear furnace in the sun's core to a higher, optically thin layer in which radiative transfer is the dominant energy transfer mechanism. Like the tropopause in planetary atmospheres, the photosphere is marked by a decrease in the lapse rate from the convectively controlled layer below to the radiatively controlled layer above.

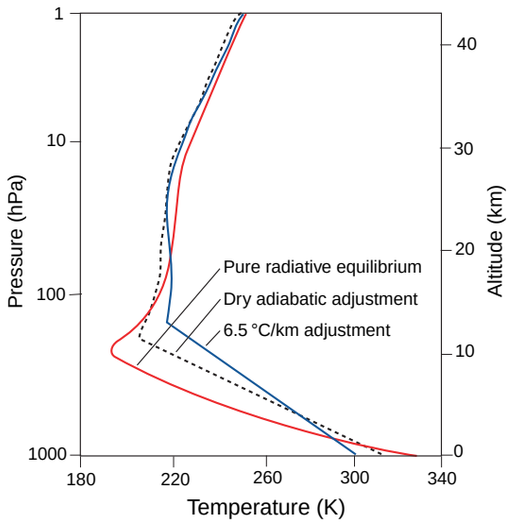

Fig. 10.4 Calculated temperature profiles for the Earth's atmosphere assuming pure *radiative equilibrium* (red curve) and *radiative convective equilibrium*, in which the lapse rate is artificially constrained not to exceed the dry adiabatic value (dashed black curve) and the observed global-mean tropospheric lapse rate (blue curve). [Adapted from *J. Atmos. Sci.*, **21**, p. 370 (1964).]

by radiative transfer, but by convection, it follows that greenhouse gases warm not only the Earth's surface, but the entire troposphere.[3]

In contrast to the troposphere, the stratosphere is close to radiative equilibrium. Heating due to the absorption of ultraviolet solar radiation by ozone is balanced by the emission of longwave radiation by greenhouse gases (mainly CO_2, H_2O, and O_3) so that the net heating rate (Fig. 4.29) is very close to zero. Raising the concentration of atmospheric CO_2 increases the emissivity of stratospheric air, thereby enabling it to dispose of the solar energy absorbed by ozone while emitting longwave radiation at a lower temperature. Hence, while the troposphere is warmed by the presence of CO_2, the stratosphere is cooled.

10.1.2 Dependence on Time of Day

As the Earth rotates on its axis, fixed points on its surface experience large imbalances in incoming and outgoing radiative fluxes as they move in and out of its shadow. As a point rotates through the sunlit, day hemisphere, the atmosphere above it and the underlying surface are heated more strongly by the absorption of solar radiation than they are cooled by the emission of longwave radiation. The energy gained during the daylight hours is lost as the point rotates through the shaded night hemisphere.

Over land, the response to the alternating heating and cooling of the underlying surface produces diurnal variations in temperature, wind, cloudiness, precipitation, and boundary-layer structure, as discussed in Chapter 9. Here we briefly discuss the direct atmospheric response to the hour-to-hour changes in the radiation balance that would occur, even in the absence of the interactions with the underlying surface. This response is often referred to as the *thermal* (i.e., thermally driven) *atmospheric tide*.[4]

Because of the atmosphere's large "thermal inertia," diurnal temperature variations within the free atmosphere are quite small, as illustrated in the following exercise. The thin Martian atmosphere reacts much more strongly to the diurnal cycle in insolation (Table 2.5).

Exercise 10.2 If the Earth's atmosphere emitted radiation to space as a blackbody and if it were completely insulated from the underlying surfaces, at what mass-averaged rate would it cool during the night?

Solution: The cooling rate in degrees K per unit time is equal to the rate of energy loss divided by the heat capacity per unit area of the free atmosphere. During the night the atmosphere continues to emit infrared radiation to space at its equivalent blackbody temperature of 255 K; hence it loses energy at a rate of

$$E = \sigma T^4 = 5.67 \times 10^{-8} \times (255)^4 = 239 \text{ W m}^{-2}$$

The heat capacity of the atmosphere (per m^2) is equal to the specific heat of dry air c_p times the mass per unit area (p/g) or

$$\frac{1004 \text{ J kg}^{-1} \text{ K}^{-1} \times 10^5 \text{ Pa}}{9.8 \text{ m s}^{-2}} \simeq 10^7 \text{ J K}^{-1} \text{ m}^{-2}$$

[3] Throughout the tropics the observed lapse-rate Γ is close to the saturated adiabatic value Γ_w. As the Earth's surface warms, the latent heat released in moist adiabatic ascent increases, and so the numerical value of Γ_w decreases. Hence, if Γ remains close to Γ_w as the tropical troposphere warms, temperatures in the upper troposphere will warm more rapidly than surface air temperature, as demonstrated in Exercise 3.45.

[4] The gravitational attraction of the moon and sun also induce atmospheric tides, but these gravitational tides are much weaker than the thermal tides.

The cooling rate is therefore

$$\frac{dT}{dt} = \frac{239\ Wm^{-2}}{10^7 Jk^{-1}\,m^{-2}} = 2.39 \times 10^{-5}\ Ks^{-1}$$

Night lasts 12 h or 4.32×10^4 s. Hence, the overnight cooling is only ~1 K. ■

The diurnal variation in incident solar radiation is not a pure sine wave: it is proportional to the cosine of the solar zenith angle during the day and zero at night (see Fig. 9.9). Because of the nonsinusoidal time dependence of the forcing, atmospheric tides are made up of an ensemble of frequencies that are integral multiples of one cycle per day. The most important of these are the *diurnal* (one cycle per day) and *semidiurnal* (two cycles per day) tides. The semidiurnal component, a response to the periodic heating and cooling of the stratospheric ozone layer, is clearly evident in tropical sea-level pressure records. The corresponding diurnal and semidiurnal variations in the horizontal wind field increase with height from ~1–2 m s^{-1} at tropospheric levels to more than 10 m s^{-1} in the mesosphere and thermosphere.

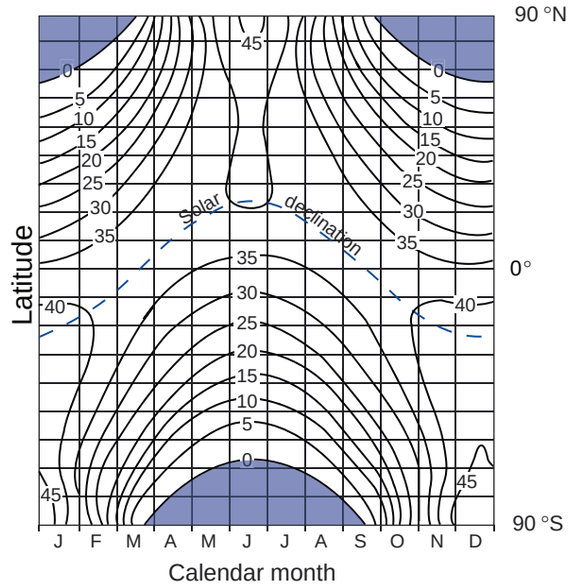

Fig. 10.5 Insolation incident on a unit horizontal surface at the top of the atmosphere, expressed in units of MJ m^{-2} integrated over the 24-h day, as a function of latitude and calendar month. Within the shaded regions the insolation is zero. To convert to units of W m^{-2} multiply the contour labels by 11.57. *Solar declination* refers to the latitude at which the sun is overhead at noon. [Adapted from *Meteorological Tables* (R. J. List, Ed.), 6th Ed., Smithsonian Institute (1951), p. 417.]

10.1.3 Seasonal Dependence

Each year, as Earth revolves around the sun, the extratropical continents experience large temperature swings and many regions of the tropics experience dramatic changes in rainfall. These periodic climate fluctuations are largely a response to the obliquity of the Earth's axis of rotation relative to the plane of the ecliptic.

The seasonally varying latitudinal distribution of insolation incident upon the top of the atmosphere is shown in Fig. 10.5. The equator-to-pole gradient is strongest during winter, when the polar cap is in darkness. In the summer hemisphere the increasing length of daylight with latitude more than offsets the increasing solar zenith angle so that insolation increases slightly with latitude. The large seasonal variations in insolation give rise to seasonally varying imbalances in net radiation at the top of the atmosphere (Fig. 10.6), which range up to 100 W m^{-2} over the subtropical and midlatitude oceans. Net radiation at the surface of the ocean (not shown) exhibits a similar distribution: upward in the winter hemisphere and downward in the summer hemisphere. Most of the excess insolation in the summer hemisphere is stored in the ocean mixed layer and the cryosphere and is released during the following winter, thereby moderating the seasonal contrast in atmospheric temperature.

The storage of heat in the ocean mixed layer is reflected in the warming of a relatively shallow layer of water near the surface during late spring and early summer, which leads to the formation of the *seasonal thermocline*, as shown in Fig. 10.7. During autumn and early winter reduced insolation and enhanced latent and sensible heat fluxes cool the mixed layer, releasing the heat that was stored during the previous summer. The warming of high latitude regions during winter by the release of this stored heat is larger than the poleward heat transport by the western boundary currents and (in the North Atlantic) by the thermohaline circulation. As the seasonal thermocline cools during autumn and winter, it also deepens by entraining water from below. The ocean mixed layer reaches its minimum temperature and maximum depth in spring, setting the stage for the redevelopment of the thermocline much closer to the ocean surface a few months later.

The large seasonal variations in the extent of polar northern hemisphere pack ice (Fig. 2.12) and other elements of the cryosphere also contribute to

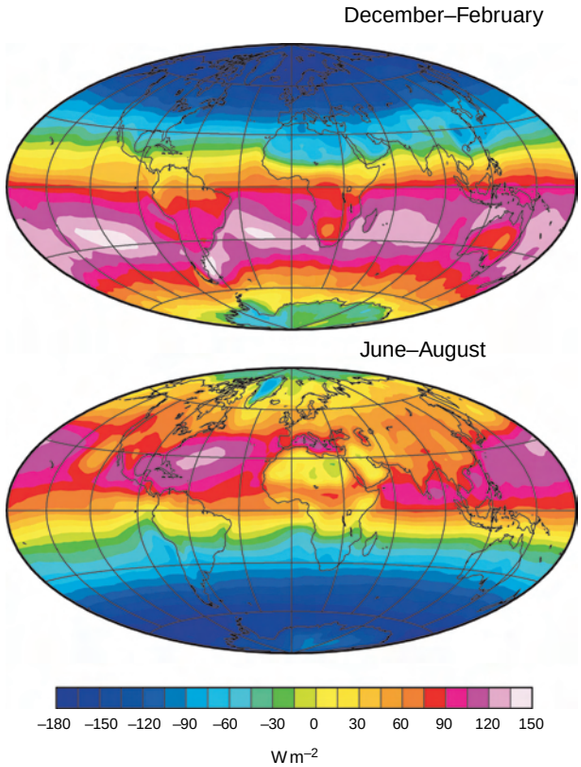

Fig. 10.6 Net radiation at the top of the atmosphere in December–February and June–August in units of W m^{-2}. [Based on data from the NASA Earth Radiation Budget Experiment. Courtesy of Dennis L. Hartmann.]

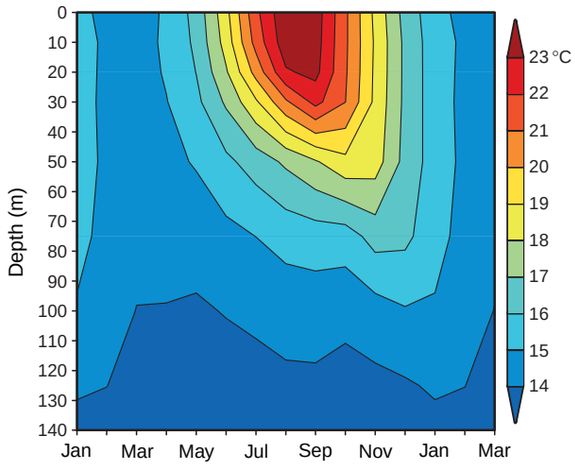

Fig. 10.7 Temperature (in °C) averaged over a region in the central North Pacific (28°–42 °N, 180°–160 °W) as a function of calendar month and depth showing the climatological-mean annual cycle. [Based on data from *World Ocean Atlas*, NOAA National Oceanographic Data Center (1994). Courtesy of Michael Alexander.]

moderating the contrast between winter and summer temperatures. Heat of fusion is taken up by the cryosphere when ice melts during the warm season. A comparable quantity of heat is released during the cold season when sea ice freezes and thickens and snow and ice particles that freeze within the atmosphere precipitate onto ice sheets and glaciers.

The large difference in the annual range of surface air temperature over the continents and oceans shown in Fig. 10.8 reflects widely differing heat capacities of the underlying surfaces. The largest ranges (~50 K) are observed over the interior of Eurasia, North America, and Antarctica, in areas far away from (or shielded by mountain ranges) from the moderating influence of the oceans.

Land–sea temperature contrasts at low latitudes of the summer hemisphere force continental-scale monsoon circulations. In analogy with Fig. 7.21, the warmth of the tropical and subtropical continents relative to the surrounding oceans in the summer hemisphere lifts the pressure surfaces and induces horizontal divergence at upper tropospheric levels, maintaining relatively low sea-level pressure over the continents relative to the surrounding oceans. The pressure contrast between land and sea drives an onshore flow of moist, boundary-layer air, triggering deep convection over land, as depicted schematically in Fig. 10.9.

In the real atmosphere the seasonally varying distribution of precipitation (Fig. 1.25) is also influenced by the land–sea geometry, the distribution of mountain ranges, and the underlying sea-surface temperature distribution. These combined influences account for distinctive regional features such as the summer rainfall maximum over the Bay of Bengal and the extensive subtropical desert regions that experience very little summer rainfall.

The tropospheric jet stream (Fig. 1.11) and the baroclinic wave activity associated with the midlatitude storm tracks tend to be strongest during wintertime, when the equator-to-pole temperature gradient is strongest.[5] At the longitude of Japan, where stationary planetary waves generated by the land–sea contrasts and the flow over the Himalayas reinforce the

[5] A notable exception is the North Pacific, where baroclinic wave activity tends to be suppressed during midwinter relative to late autumn and early spring.